Journal of Sound and Vibration (1999) **225**(1), 189–200
Article No. jsvi.1999.2213, available online at http://www.idealibrary.com IDEAL®

LETTERS TO THE EDITOR

SCALING CONCEPTS IN RANDOM ACOUSTIC FATIGUE TESTING

MARTY FERMAN

Aerospace and Mechanical Engineering Department, Parks College, St. Louis University, 3450 *Lindell Blvd, St. Louis, MO* 63156, *U.S.A.*

AND

HOWARD WOLFE

Air Force Research Laboratory, Wright Patterson AFB, OH 45433, *U.S.A.*

(*Received* 7 *October* 1997, *and in final form* 16 *February* 1999)

1. BACKGROUND

While it is important to continually expand the capability of acoustic test facilities, it is perhaps equally important to be able to work with existing facilities at any time in terms of economy and speed of testing. Facility expansions, enhancements, and modernizations should always be sought from time to time, so long as practical and affordable from cost effectivity. Limits should be pushed to accommodate larger test specimens at higher noise levels, with wider ranges of frequencies, with wider ranges of temperatures, and with better capabilities for applying pressures along with any one of several types of preloads. Facility rental can be used in some cases to bolster one's testing facilities. However, if the application suggests a situation beyond the available facility capability for the required design proof, then an alternate is needed, especially if results are needed quickly. Thus, the scaling concept suggested here is a viable and useable possibility. This paper extends recent work by the writers on this scaling concept [1].

The author's basis for the approach stems from their extensive, collective, experience in structural dynamics (some 72 + years), especially work in acoustic fatigue, fluid–structure interaction, buffet, and aeroelasticity/flutter. In particular, experience with flutter model testing, in which it is quite common to ratio test results from a model size to full scale for valid predictions, makes the present approach quite appealing. Flutter model data is commonly used in non-dimensional form to establish design margins of safety [2–4]. Flutter can be non-dimensionalized broadly, as noted in many works, especially with the simplified flutter concept [4]. The degree of the use of the flutter model scaling rules varies considerably today, because some people are testing as much or more than ever, while others are testing less and relying more heavily on advanced theories such as computational fluid dynamics (CFD). These flutter models provide a safety check for full-scale flight tests, and help economize testing by aiding the test plan and matrix of test conditions. This concept has fuelled the author's desire to

0022-460X/99/310189 + 12 $30.00/0

develop the "acoustical scaling" used herein. Similarly, the authors realize that scaling is also common to many related areas of structural dynamics, and thus refer to two other cases herein.

For example, in fluid–structure interaction and fatigue of fuel tank skins, scaling was used to demonstrate accurate predictions with widely varied environmental levels, and a multitude of configurations [5–14]. This extensive work showed that for several configurations for several panel thicknesses for widely varying environmental input, panel response and fatigue could be collapsed into design charts using non-dimensional trends. This work also showed that both linear and non-linear data could be treated accurately. In retrospect, hindsight now suggests that there is a clear relation between the scaling approach used there and the scaling approach used herein.

It is now well reconized that buffet is easily scaled. Many engineers and investigators are now employing scaling of pressures from model to full size applications, and are also using scaled model response to predict full-scale cases. Some of the earliest work by Ducan and Frazer [15] used modelling, and some of the most modern results clearly show this aspect [16–18]. Buffet models, a fraction of full scale, are commonly being used to scale model scale measured buffet pressures for analysis, and to scale model response data to guide full-scale flight tests. These results with models show excellent correlation with full-scale flight test through the use of non-dimensional parameters, such as bending moment coefficient for example. Besides giving full-sized results, providing a guide to safe flight testing, these models offer a means to economize the full-sized tests by aiding with the test condition matrix.

Obviously, acoustical response and fatigue phenomenon are also non-dimensionalizable and scaleable [19, 20], for example. This point is being taken further here, that is, scaling will be used to take better advantage of limited facility testing capability to predict more severe situations, as is used in the case of flutter model testing where a larger specimen is predicted from tests of a smaller structure using similarity rules. Here in the acoustic application, a thinner, or otherwise more responsive specimen, is tested and then analytical means are used to make the prediction for the nominal case.

2. APPROACH

The method shown here is basically an extension of the flutter model scaling idea, as applied to acoustical fatigue testing with a particular emphasis on random applications. The technique will also work for sine type testing in acoustical fatigue, and perhaps it will be even more accurate there, but most of today's applications are with random testing, notably in the aircraft field. Thus it is in this area where the method should find more application. It is believed that the best testing for random acoustic fatigue is, of course, with (1) the most highly representative structure, and as large a piece as can be tested, both practically and economically, (2) the most representative environmental levels in both spectrum shape and frequency content, (3) test times to represent true or scaled time, as commonly accepted,

(4) temperatures should be applied both statically and dynamically, and finally (5) preloading from pressures, vibration, and from boundary loading of adjacent structure. Frequently, testing is done to accomplish some goal using a portion of these factors, and the remainder is estimated.

The authors believed that there is a high potential to extend the flutter model approach to acoustical applications. Recall that in the flutter model approach, the full-scale flutter speed is predicted by the rule

$$((V_F)_A)_P = [((V_F)_M)_E/((V_F)_M)_C] \times [((V_F)_A)_C], \tag{1}$$

where V_F is the flutter speed, the subscripts M and A refer to model and aircraft respectively, the subscript C refers to calculated, E refers to experimental, and the subscript P refers to predicted. Thus, the equation suggests that the full-scale predicted flutter speed is obtained by taking the ratio of experimental to calculated flutter speed for the model and then multiplying by a calculated speed for the airplane. These flutter model scaling ideas are covered in any number of references, i.e. references [2–4] for example.

The same concept can be utilized in acoustic fatigue, i.e. the strain value and cycle count at fatigue failure, (ε, N), can be scaled from model structure tested at one level and then adjusted for structural sizing and environmental levels. This relation can be addressed as done for the flutter case:

$$((\varepsilon, N)_A)_P = [((\varepsilon, N)_M)_E/((\varepsilon, N)_M)_C] \times [((\varepsilon, N)_A)_C], \tag{2}$$

where ε is the strain, and N is the number of cycles at failure, where as above in equation (1), the subscripts M and A refer respectively to model and full scale for parallelism, while the subscripts E, C, and P have the same connotation again, namely, experimental, calculated, and predicted. Thus, the full-scale case is predicted from a subscale case by using the ratio of experimental to theoretical model results as adjusted by a full-scale calculation.

Flutter model scaling depends upon matching several non-dimensional parameters to allow the scaling steps to be valid. Similarly, parameters unique to this acoustical application must be considered, and will be discussed. Accurate predictions for the method relies on extensive experience with the topic of Acoustic Fatigue in general, because concern is usually directed towards the thinner structure such as panels, panels and stiffeners, and panels and frames, bays (a group of panels), or other substructure supporting the panels. These structures are difficult to predict and are quite sensitive to edge conditions, fastening methods, combination of static and dynamic loading, and temperature effects. Panel response predeiction is difficult, and the fatigue properties of the basic material in the presence of these complex loadings is difficult. However, the experienced acoustic fatigue engineer is aware of the limits, and normally accounts for these concerns. Thus, the method here will show that these same concerns can be accounted for with the scaling approach through careful considerations.

The author's method is best explained by reviewing the standard approach to acoustic fatigue, especially when facility limits are of major concern (Figure 1).

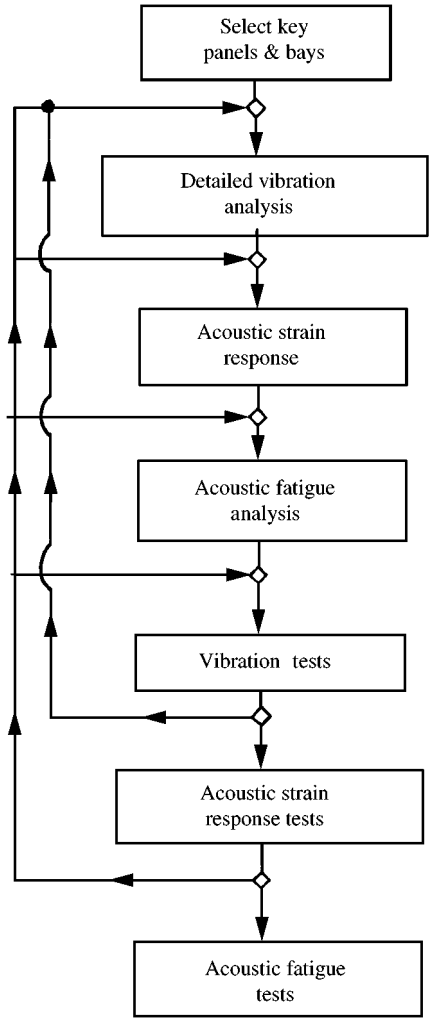

Figure 1. Standard acoustic fatigue method.

Key panels for detail design are selected from a configuration, where the combination of the largest, thinnest, and most severely loaded panels at the worst temperature extremes and exposure times are identified. These can be selected by many means, i.e., empirical methods, computational means, and government guides [19, 20]. Detailed vibration studies are run using finite elements, Rayleigh methods, finite-difference methods, etc., to determine the modal frequencies and shapes, and frequently linearity is assessed. Then acoustical strain response is determined for sine, narrowband, and broadband random input to assess fatigue life based on environmental exposure times in an aircraft lifetime of usage. Vibration tests are run for the worst cases, where modal frequencies, shapes, and damping, and linearity are checked. This is followed by acoustical strain response tests where the strain growth versus noise levels is checked, employing sine, narrowband and broadband random excitation. Data from the vibration tests are fed back to the

theoretical arena to update studies and to correlate with predictions, especially damping, and of course, the representation of non-linearity. Also, the measured strain response is again used to update fatigue predictions. These updates to theory are made before the fatigue tests are run to insure that nothing is missed.

The new concept of scaled acoustic fatigue structures is shown on the sketch of Figure 2 where the standard method is again indicated in summary, to refocus the thrust of the new idea. The scaling process parallels, and complements, the standard approach, so that the two can be run simultaneously to save time, costs, and manpower. Here the panel selection process recognizes that the design application requires environments far in excess of available facility capability. Thus, the scaling is invoked in the beginning of the design cycle. As the nominal panels (bays) are selected and analyzed for vibration, response and fatigue, scaled structures are defined to provide better response within the existing chamber ranges so that they can be fatigued and then the results can be rescaled to the nominal case. In this manner, appropriate designs can be established to meet safety margins with more confidence, and will avoid costly redesign and retrofitting at downstream stages where added costs can occur and where down times are difficult to tolerate.

The concept is further illustrated hypothetically in the sketch of Figure 3, where the test facility cannot produce the highest noise level needed for a nominal case, and thus a second configuration, a scaled, thinner, model is used to obtain results. Here the strain response curve of the nominal case and that of the scaled version are combined with strain to failure data (coupon tests) to predict fatigue results. The scaled model being thinner is more responsive and shows the upper response curve. Note, the test-based strain response for the nominal case at the highest SPL level available gives the fatigue value at point A on the coupon curve, while fatigue data is needed at the higher SPL level, which is not available directly. This higher level case is attainable only by extrapolation of the test data, indicating point B on the fatigue curve. There is a much higher level of response at the upper SPL limit of the facility for the scaled model, thus indicating the fatigue result at point C. Ideally, when rescaled point C should match point B, but assuming some typical error between theory and test and with test scatter, gives point D which differs slightly from the extrapolated point B as it most likely will, realistically. More faith should

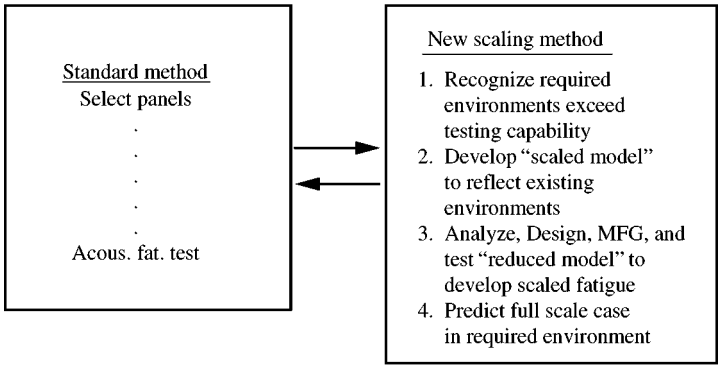

Figure 2. Scaling method fits-in with general design cycle for acoustic fatigue.

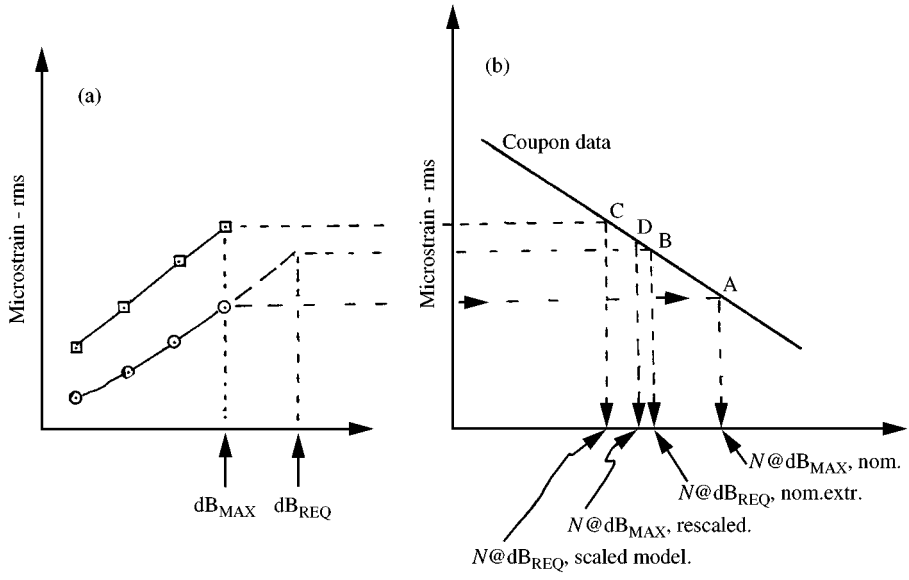

Figure 3. Hypothetical example of acoustic scaling to tests at higher SPLs. ⊡, scaled model; ⊙, nominal model; – – – – –, nominal model, extrapolated. (a) Sound Pressure level in dB, (b) N cycles to failure.

be placed on data from an actual fatigue point than a point based on the projected strain response curve. This is the power of the method, using two experimental response curves and two analyses to predict the fatigue point normally estimated by extrapolation. The interplay between the two models on the fatigue curve will be accomplished with equation (2), while more analytics are given below in a more detailed example.

Figure 4 illustrates the winning virtue of the scaleable design. First, the figure shows a hypothetical set of acoustical fatigue test data (ε, N) obtained at various SPLs for two structural designs, a nominal case and a scaled version. This is an elaboration of Figure 3, where the authors have scattered data with typical behavior patterns based on their extensive experience. The nominal case is shown by open circles, and the anticipated results from extrapolation to higher SPLs are shown by flagged open circles. The scaled model results are shown by closed squares, and the rescaled data by flagged, closed squares. The scaled model was assumed to be thinner here for example, and the test results for that model are again rescaled to compare with the nominal case results. The most interesting aspect is shown by the two clusters of data, denoted as **A** and **B** where there are rough circles drawn about the clusters. Here the emphasis is that tests of the scaled model are used to find the higher strain conditions which cannot be found from the nominal case. In circle **A**, the scaled model results are compared to those anticipated by the extrapolated nominal case. In both cases at the highest strain levels, the facility is used to its limits, but with enough testing with the thinner case, adequate data is available to make the prediction more accurate using equation (2) for the final correlation as shown here. In circle **B**, the rescaled model data is compared to the

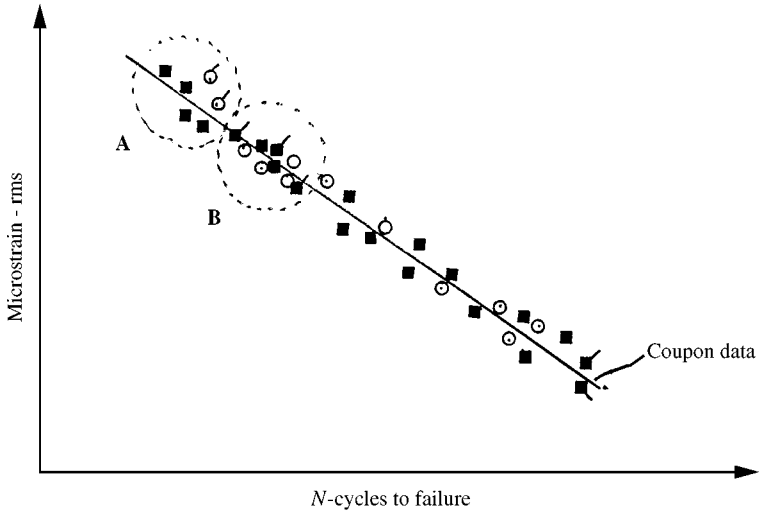

Figure 4. Statistical aspects of scaling for hypothetical fatigue cases. nominal model: ○, tests; ◜, extrapolated. Scaled model: ■, tests; ◤, rescaled, equation (2).

nominal case tests for further corroboration of the data. The statistical scattering of the scaled data will be an accurate measure for the nominal case, particularly when compared to estimates based on extrapolation of the strain response for the nominal case. There are many cautions to be noted with this approach as there are with all acoustic fatigue methods, and of course, tests. First, the linearity of the modes, either in unimodal sine excitation, multi-mode sine, narrowband or broadband random must be carefully handled. The strain response of individual locations throughout the structure must be carefully monitored in calculations and tests so that strain response is truly understood and used to define fatigue life carefully. This is difficult to do in many applications where widely varying conditions and durations require some type of Miner Rule combination to provide a true measure of fatigue.

Similarly, strain risers at fasteners, discontinuities, holes, frames, stiffeners, material changes, along with temperature gradients and temperature transients, require final "tweeks" to predictions, regardless. Non-linearity, especially in the multi-mode case, is one of the most formidable foes to conquer for any application.

3. APPLICATIONS AND EXAMPLES

The tests of an Aluminium panel, 7075-T6, of size of 10×20 in and with a thickness of 0·063 in [21] will be used to illustrate the technique. The panel has approximately fixed–fixed edge conditions. Strain responses were measured for this panel to a SPL of 164 dB, the facility limit. One fatigue point was found for this panel at the 164 dB limit [22]. For this example, it is assumed that strain response and fatigue data were needed at 175 dB for the 0·063 in panel, which is above the facility limit. To show the new technique, it was assumed that a panel of the same size and material, but of a thickness of 0·040 in could be tested and used to

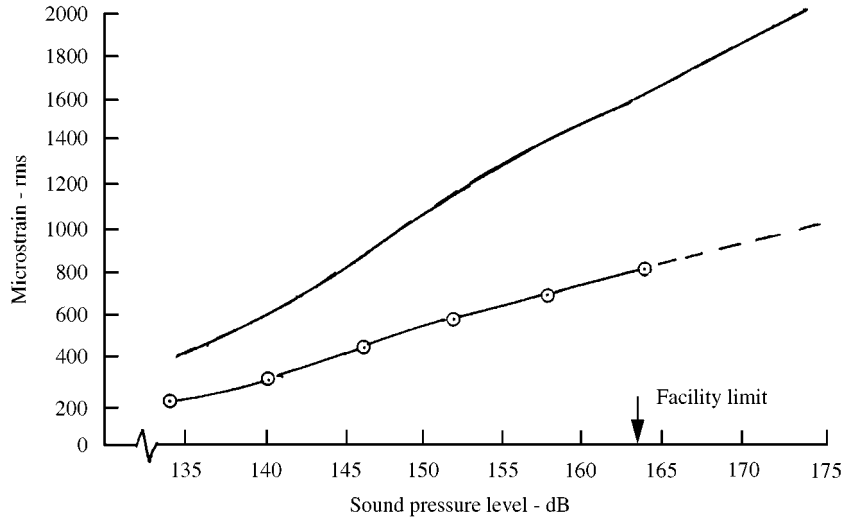

Figure 5. Strain response of aluminum panels ($10 \times 20 \times 0{\cdot}063$ in., 7075 T(6), narrowband random excitation: ——, calculated for 0·040 panel; ⊙, tests for 0·063 panel [21]; – – –, extrapolated for 0·063 panel.

find the fatigue at 175 dB. However, since no test was actually available, calculations were substituted. The measured strain response for the 0·063 in panel is shown in Figure 5 along with the calculated response curve for the thinner panel (0·040 in). The strain response for the thinner case was calculated using the equations below. The panel deflection, z, is given in terms of amplitude of plate response, δ, and mode shape, $z = \phi\delta$, where the amplitude is given as

$$\delta = \frac{\left[\iint \phi^2 \, \mathrm{d}x \, \mathrm{d}y\right][PSD_P(f)]}{M\omega_n^{3/2}(8\zeta)^{1/2}}, \tag{3}$$

where M is the generalized mass, ω_n is the natural frequency, ζ is the viscous damping factor, ϕ is an assumed mode shape, PSD_P is the pressure power spectral density, and x, y are the positional co-ordinates along the plate from a corner. Using the elastic energy equation for plates from Timoshenko [23], and the approximate mode shape for the first mode of a fixed–fixed plate,

$$\phi = \left(\frac{1}{4}\right)\left(1 - \cos\left(\frac{2\pi x}{a}\right)\right)\left(1 - \cos\left(\frac{2\pi y}{b}\right)\right). \tag{4}$$

Then, the approximate expression for the natural frequency of the first mode by application of the Rayleigh method is

$$\omega_n = \left(\frac{4\pi^2 t}{3a^2}\right)\sqrt{\frac{Eg\left(3\,\frac{a^4}{b^4} + 2\,\frac{a^2}{b^2} + 3\right)}{12\rho_w(1-\mu^2)}}. \tag{5}$$

Since strain, ε, is proportional to the amplitude, the maximum strain in x is ε_{xx}, or

$$\varepsilon_{xx} = (t/2)(\partial\phi^2/\partial x^2)\delta \tag{6}$$

and by combining equations (3–6) shows that the strain response ε_{xx} can be given by

$$\varepsilon_{xx} = 16ag^{1/4}\left[\frac{PSD_P(f)}{8\varsigma}\right]^{1/2}\Bigg/\left\{9\pi\left(\frac{4}{3}\right)^{3/2} t^{3/2}\rho_W^{1/4}\left[\frac{E\left(3\dfrac{a^4}{b^4} + 2\dfrac{a^2}{b^2} + 3\right)}{12(1-\mu^2)}\right]^{3/4}\right\}. \tag{7}$$

assuming $a < b$, this is the maximum strain at the middle of the longer side at the edge, where $x = 0$. For this example, the only difference between the two panels is thickness, thus the strain response of the two panels (and the curves) differ only by the thickness factor ratio given by

$$\varepsilon_2 = \varepsilon_1(t_1/t_2)^{3/2}. \tag{8}$$

However, it must be noted that the 0·063 panel exhibited non-linear behavior [21], and thus, the direct application of the linear response equations is not exactly correct, but simply used for an illustration here.

From Figure 5, the data for the 0·063 thickness is extrapolated to the required SPL of 175 dB, showing a strain of 1000 μ in/in. The calculated curve for the thinner panel of 0·040 in. shows a greater response at all dB levels as it should, and moreover shows that only 150 dB are needed to achieve the 1000 $\mu\varepsilon$ condition. (Moreover, the thinner panel will exhibit large enough strains at the lower SPLs to improve the fatigue curve where the thicker panel is insensitive.)

Taking the example a step further, the fatigue properties for these two panel thicknesses are shown on a strain to failure plot (ε versus N) in Figure 6, along with a beam coupon data line [12], as these coupons were shown to correlate closely with a large number of panel test points [7–14]. The nominal data is shown by triangles in the figure. The predicted fatigue point for the nominal case at a SPL of 164 dB at 800 $\mu\varepsilon$ is shown by open symbol versus that measured by a closed symbol. Note that the test required a slightly larger time, reflected in the N values, suggesting predictions are slightly conservative, a positive design safety factor. The estimated fatigue point for the 0·063 case when extrapolating strain response to a SPL of 175 dB at 1000 $\mu\varepsilon$ is shown by the flagged triangle. Open circles show predicted fatigue points for the 0·040 panel for SPLs of 150, 164 and 175 dB. Note that the fatigue for the thinner panel at the SPL of 150 dB at 800 $\mu\varepsilon$ requires slightly more time due to lower frequency for the thinner panel. The actual fatigue point at 164 dB for the nominal case required 3 h and was predicted to be 2·8 h. Using the experimental to predicted strain ratio from equation (2) for the 0·063 panel application, the result for the 0·040 panel is adjusted to the right a little more; see the flagged symbol as a rescaled point. The estimated fatigue for the extrapolated case of 175 dB was estimated to be 1·7 h, while the scaled point from the thinner

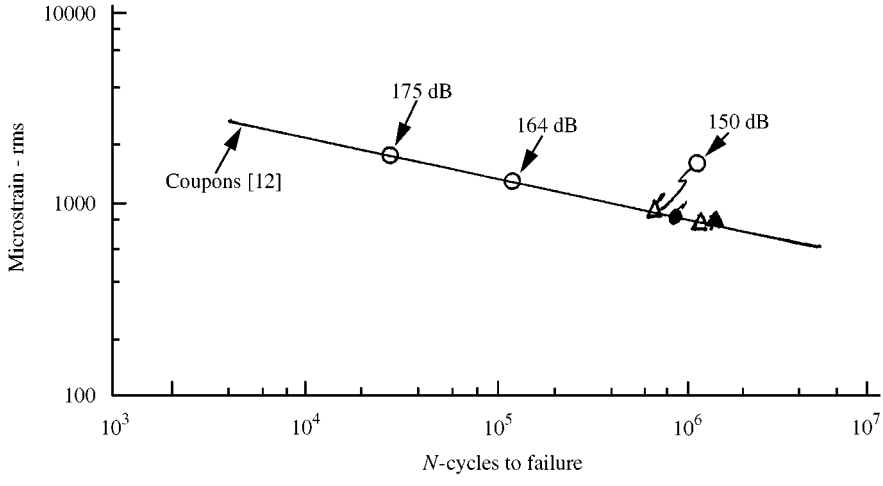

Figure 6. Fatigue example of the 10×20 in aluminium panels. 0·063 Panel: △, predicted at 164 dB; ▲, measured at 164 dB; ◭, extrapolated at 175 dB. 0·040 Panel: ○, scaled result; ●, rescaled, equation (2).

panel was estimated to be 2·2 h which is slightly off, using equation (2), but the authors have had to rely on log plots for much of the data and thus lack some accuracy. The success of using a thinner panel at existing SPLs is thus demonstrated here.

4. CONCLUSIONS AND RECOMMENDATIONS

An attempt was made to employ a view of acoustical scaling different from that usually taken. The idea is to develop data for a model that fits within a test facility's capability and then by using analytical methods, adjust these results to the nominal case using factors based on the ratio of experimental to calculated data for the test specimen. This is analogous to the flutter model approach. One example is offered, and similar results from related scaling in fluid–structure and buffet work were noted to further the point. While more work is needed to fully display the concept, enough has been done to inspire others to dig-in to more fully evaluate the approach. The writers fully intend to do more, since they truly appreciate this difficult task. One must be careful here, because there can be subtle differences between theory and test, and this can mislead inexperienced persons applying these methods. A number of other reminders are given throughout this paper to caution that this topic of acoustic fatigue is not for the novice, but rather requires a great deal of experience to be successful in application and design.

REFERENCES

1. M. Ferman and H. Wolfe 1997 *6th International Conference on Recent Advances in Structural Dynamics, University of Southampton, ISVR, Southampton, U.K.* 14–17 *July*. Scaling concepts in random acoustic fatigue.

2. R. H. Scanlon and R. Rosenbaum 1951 *Introduction to the Study of Aircraft Vibration and Flutter*. New York: The MacMillian Company.
3. R. L. Bisplinghoff, H. Ashley and R. L. Halfman 1995 *Aeroelasticity*, 695–787, Reading, MA: Addison-Wesley.
4. M. A. Ferman 1967 *Conceptual Flutter Analysis Techniques – Final Report*, *Navy BuWeps Contract no. w* 64-0298-*c*, *McDonnell Report F*322, 10 *February*.
5. M. A. Ferman and W. H. Unger 1979 17*th Aerospace Sciences Meeting*, *New Orleans*, *LA*, *January*. Fluid–Structure interaction dynamics in fuel cells.
6. M. A. Ferman, and W. H. Unger 1979 *AIAA Journal of Aircraft* Fluid–Structure interaction dynamics in aircraft fuel cells, December.
7. M. A. Ferman *et al.* 1982 *USAF AFWAL TR*-83-3066, *WPAFB*, *OH*. Fuel tank durability with fluid–structure interaction dynamics, September.
8. M. A. Ferman, W. H. Unger, C. R. Saff and M. D. Richardson 1985 A new approach to durability predictions for fuel tank skins. 26th SDM, Orlando, FL, 15–17 April 1985.
9. M. A. Ferman, W. H. Unger, C. R. Saff and M. D. Richardson 1986 *Journal of Aircraft* **23**, A new approach to durability prediction for fuel tank skins.
10. C. R. Saff, and M. A. Ferman 1985 *ASTM Symposium of Fracture Mechanics*, *Charleston*, *SC*, 21 *March*. Fatigue life analysis of fuel tank skins under combined loads.
11. M. A. Ferman, M. D. Healey, W. H. Unger and M. D. Richardson, 1986 27*th SDM*, *San Antonio*, *TX*, 19–21 *May*. Durability prediction of parallel fuel tank skins with fluid-structure interaction dynamics.
12. M. A. Ferman and M. D. Healey 1987 *AFWAL TR*-87-3066, *Wright-Patterson AFB*, *OH*, *November*. Analysis of fuel tank dynamics for complex configurations.
13. M. A. Ferman, M. D. Healey and M. D. Richardson 1988 29*th SDM*, *Williamsburg*, *VA*, 18–20 April. Durability prediction of complex panels with fluid-structure interaction.
14. M. A. Ferman, M. D. Healey and M. D. Richardson, 1989 *AGARD/NATO* 68*th SMP*, *Ottawa*, *Canada*, 23–28 *April*. A dynamicist's view of fuel tank skin durability.
15. R. A. Frazer and W. J. Duncan 1931 *BR R&M* 1360. The accident investigation subcommittee on the accident to the Airplane G-AAZK at Mepoham, Kent, England.
16. N. H. Zimmerman and M. A. Ferman 1987 *USN Report*, *NADC* 88043-30, July. Prediction of tail buffet loads for design applications.
17. N. H. Zimmerman, M. A. Ferman and R. N. Yurkovich 1989 30*th SDM*, *Mobil*, *AL*, 3–5 *April*. Prediction of tail buffet loads for design applications.
18. M. A. Ferman, S. R. Patel, N. H. Zimmerman and G. Gersternkorn 1990 *AGARD/NATO* 70*th SMP*, *Sorrento*, *Italy*, 2–4 *April*. A unified approach to buffet response of fighter aircraft empennage.
19. M. J. Cote *et al.* 1963 *USAF ASD-TR*-63-820, *WPAFB*, *OH*, *October*. Structural design for acoustic fatigue.
20. F. F. Rudder and H. E. Plumblee 1975 *AFFDL-TR*-74-112, *Wright-Patterson AFB*, *OH*, *May*. Sonic fatigue guide for military aircraft.
21. J. H. Jacobs and M. A. Ferman 1994 *AGARD/NATO SMP*, *Lillehammer*, *Norway*, 4–6 *May*. Acoustic fatigue characteristics of advanced materials and structures.
22. McDonnell Douglas Lab Report, Tech. Memo 253.4415. 1984 Acoustic fatigue tests of four aluminum panels, two with polyurethene sprayon.
23. S. Timoshenko and S. Wionowsky-Krieger 1959 *Theory of Plates and Shells*, 344. New York: McGraw-Hill, Inc.

APPENDIX: NOTATION

a	panel width along the x direction, $a < b$
b	panel length along the y direction
CFD	computational fluid dynamics

E	Young's modulus
f	frequency in Hz (cycles per second)
g	gravity, 32·2 ft/s^2
M	mass, generalized
N	number of cycles
PSD	power spectral density
V	velocity
t	panel thickness
x, y	positional co-ordinates along panel edges
z	panel deflection
δ	panel amplitude of response
ε	panel strain
ϕ	panel mode shape
μ	the Poisson ratio
ρ	weight density
ω	natural frequency, rad/s
∂	partial derivative

Subscripts

A	full scale or prototype
C	calculated
E	experimental
F	flutter
M	model
n	natural
p	pressure
P	predicted